

Received 27 June 2022, accepted 2 August 2022, date of publication 10 August 2022, date of current version 16 August 2022.

Digital Object Identifier 10.1109/ACCESS.2022.3197889

RESEARCH ARTICLE

Effects of Carbon Incorporation on Electrical Characteristics and Thermal Stability of Ti/TiO₂/n-Ge MIS Contact

IKSOO PARK¹, (Student Member, IEEE), SEONGHWAN SHIN¹, (Student Member, IEEE),
JUNGSIK KIM², (Member, IEEE), BO JIN³, (Member, IEEE),
AND JEONG-SOO LEE¹, (Senior Member, IEEE)

¹Department of Electrical Engineering, Pohang University of Science and Technology (POSTECH), Pohang-si 37673, South Korea

²Department of Electrical Engineering, Gyeongsang National University, Jinju-si 52828, South Korea

³Research and Development Department, IGEST—Innovative General Electronics Sensor Technology Company Ltd., Pohang-si 37673, South Korea

Corresponding authors: Jeong-Soo Lee (ljs6951@postech.ac.kr) and Bo Jin (jinshengzhi1986@sina.com)

This work was supported in part by the National Research and Development Program through the National Research Foundation of Korea (NRF) funded by the Ministry of Science and ICT under Grant 2020M3H2A1078045, and in part by the Samsung-POSTECH Research Center (SPRC) funded by Samsung Electronics under Grant IO201211-08125-01.

ABSTRACT The effects of carbon incorporation on the thermal stability of the interfacial TiO₂ layer and the electrical characteristics of Ti/TiO₂/n-Ge contacts were investigated. The improved thermal stability and contact characteristics of Ti/TiO₂/n-Ge contacts were characterized in terms of Schottky barrier height (SBH) and specific contact resistivity (ρ_c) using the Schottky diode and circular transmission line model (CTLM). The values of SBH and ρ_c increased after the rapid thermal annealing (RTA) above 550 °C. The current density–bias voltage ($J - V$) curves of the Schottky diode showed a change of contact characteristics from Ohmic-like behavior to rectifying. This thermal instability was mainly caused by the decomposition of the interfacial TiO₂ layer after high-temperature annealing. The structural degradation was confirmed by transmission electron microscopy (TEM) and electron energy loss spectroscopy (EELS) analyses. When carbon ions were incorporated into the interfacial TiO₂ layer, the SBH and ρ_c values showed relatively stable characteristics as the RTA temperature increased up to 600 °C. The EELS mapping showed that the diffusion of oxygen from the interfacial TiO₂ layer was effectively suppressed thanks to the incorporation of carbon. Thus, the carbon incorporation can improve the thermal stability of the interfacial TiO₂ layer and the metal–insulator–semiconductor contact characteristics for Ge-based device applications.

INDEX TERMS Germanium, metal–insulator–semiconductor, thermal stability, Schottky barrier height, Fermi-level pinning, contact resistivity.

I. INTRODUCTION

Germanium (Ge) has been introduced as a promising replacement for silicon (Si) as a channel material in future complementary metal–oxide–semiconductor (CMOS) devices owing to its high carrier mobility and high compatibility with the advanced Si device fabrication technology [1], [2], [3]. However, the formation of source and drain (S/D) contact with a low contact resistance is a major bottleneck in

The associate editor coordinating the review of this manuscript and approving it for publication was Zhe Zhang¹.

the commercialization of Ge-based devices. This is mainly attributed to the solid solubility and diffusivity issues of *n*-type dopants in Ge and the Fermi-level pinning (FLP) effect [4], [5], [6]. The FLP effect originates from the metal-induced gap states (MIGS) in the vicinity of a metal/Ge interface. Because it causes near the valence band (E_v) of Ge, it increases Schottky barrier height (SBH) to above 0.5 eV regardless of the metal work function [7], [8], [9].

In recent years, metal–insulator–semiconductor (MIS) contact has been proposed to mitigate the FLP effect. As an ultrathin insulator is inserted between metal and

semiconductor as an interfacial layer, the penetration of the electron wave function from a metal into a semiconductor could be reduced; this suppresses the FLP effect [10], [11]. Among several high- k dielectrics, titanium dioxide (TiO_2) is a promising candidate as an interfacial layer of MIS contact because of its negligible conduction band offset (CBO) on an n -Ge (100) substrate and its relatively high conductivity, which contributes to the low tunneling resistance of MIS contacts [12], [13], [14]. However, considering that the high thermal budget process after the formation of S/D contact such as conventional back-end-of-line (BEOL) processes, the thermal stability of MIS contacts in the n -Ge device must be guaranteed above 400 °C to achieve the low S/D contact resistance.

Several manners have been reported to improve the thermal stability of MIS contacts, for instance, nitrogen plasma treatment and hydrogen annealing [15], [16], [17]. Also, carbon implantation (C-imp) has been utilized to achieve low specific contact resistivity (ρ_c) values and to improve the thermal stability of alloying metal–semiconductor (MS) contacts such as silicide and germanide. Besides, C-imp could enhance dopant segregation and reduce FLP in Ti/Ge contacts [18].

In this work, we investigated the effects of carbon incorporation on the thermal stability of the interfacial TiO_2 layer of MIS contact and the electrical characteristics of Ti/ TiO_2 / n -Ge contacts at thermal annealing temperatures of 450–600 °C. The structural characterization of the interfacial TiO_2 layer was analyzed using transmission electron microscopy (TEM) and electron energy loss spectroscopy (EELS). Schottky diodes and a circular transmission line model (CTLTM) were used to characterize the contact characteristics and thermal stability of Ti/ TiO_2 / n -Ge contacts with carbon incorporated TiO_2 layer.

II. EXPERIMENTAL METHODS

Schottky diodes and CTLTM test structures were fabricated on n -type Ge substrate to analyze the contact characteristics of Ti/ TiO_2 / n -Ge such as SBH and ρ_c , respectively. The detailed fabrication flow has been described as follows: moderately doped n -type 4-inch Ge (100) wafers ($\sim 10^{18} \text{ cm}^{-3}$) were used as starting materials. The wafers were cleaned with acetone and rinsed with deionized (D.I.) water. And then, the wafers were dipped in 2% diluted hydrofluoric acid (dHF, HF: $\text{H}_2\text{O} = 1:50 \text{ ml: ml}$) in order to remove native oxides and rinsed with D.I. water. First, a 100-nm-thick SiO_2 layer was deposited using plasma-enhanced chemical vapor deposition (PECVD) to isolate the contact holes where the pressure, RF power, and temperature were 8 mTorr, 600W, and 300 °C. Subsequently, the Schottky diode and CTLTM test structure were patterned using photolithography for micron patterns and an i-line stepper for the sub-micron patterns, respectively. Sequentially, the patterned PECVD oxide was etched using a dry etcher, and the interfacial TiO_2 layers were deposited using atomic layer deposition (ALD) to create an MIS structure. The precursors for the ALD TiO_2 layer were tetrakis(dimethylamido)titanium (TDMA-Ti) and H_2O .

The atomic deposition of TiO_2 layers was performed with 50 cycles at 200 °C atmospheres to form a 2-nm-thick layer.

Next, carbon ions were implanted into the interfacial TiO_2 layer in order to form a diffusion barrier of oxygen ions and to amorphize the surface using an ion implanter (Nissin Ion, Impheat). And the ion implantation condition is as follows: An implantation dose of 10^{15} cm^{-2} , implantation energy of 10 keV, and a tilt angle of 7°. The optimal ion implantation condition has been established considering the series resistances of Ti/ TiO_2 / n -Ge contacts. Then, Ti (5 nm)/TiN (5 nm) layers were deposited using a DC sputtering system. Thereafter, heat treatment was carried out in N_2 ambient for 60 s at 450–600 °C using RTA.

After the fabrication of Schottky diodes and CTLTM test structures, the electrical characteristics were analyzed using Keithley 4200-SCS. The current density–bias voltage ($J - V$) curves of Schottky diodes were measured, and the values of SBH were calculated using the current-temperature ($I - T$) method. Also, the ρ_c values of Ti/ TiO_2 / n -Ge contacts were extracted using the transfer length method (TLM).

Preparing the specimens for the TEM and EELS analyses was performed using a dual-beam focused ion beam (Dual-FIB) with Ga^+ ion beam milling and thinning at 30 kV acceleration voltage. Then, conventional TEM images and EELS maps of Ti/ TiO_2 / n -Ge contacts with and without C-imp were obtained using a JEOL JEM 2200FS with an image Cs-corrector.

III. RESULTS AND DISCUSSION

Fig. 1 shows the reverse current density (J_{OFF}), which is measured under bias condition: $V = -2.0\text{V}$, of the Ti/ TiO_2 / n -Ge Schottky diode with and without C-imp as a function of the annealing temperature. The insets show the $J - V$ characteristics of Ti/ TiO_2 / n -Ge diode with and without C-imp. The J_{OFF} values with and without C-imp after RTA at 450 °C show an Ohmic behavior due to alleviation of FLP by inserting the interfacial TiO_2 layer. However, as the annealing temperature increases, J_{OFF} without C-imp decreases significantly, but the J_{OFF} with C-imp was almost consistent. In other words, the Ti/ TiO_2 / n -Ge Schottky diode with C-imp shows stable Ohmic characteristics after high-temperature annealing. On the other hand, the Ti/ TiO_2 / n -Ge Schottky diode without C-imp shows the non-linear characteristic, which is attributed to the poor thermal stability of TiO_2 mainly due to the out-diffusion of oxygen [19], [20], [21].

The SBH values have been extracted from the current-temperature ($I - T$) curves of Ti/ TiO_2 / n -Ge Schottky diodes with and without C-imp for 27–105 °C. The $I - V$ relationship for fabricated Schottky diodes is represented by [22]

$$I = AA^* e^{-q\phi_B/kT} \left(e^{qV/nkT} - 1 \right) = I_s \left(e^{qV/nkT} - 1 \right) \quad (1)$$

where I_s is the saturation current, A is the diode area, $A^* = 4\pi qk^2 m^*/h^3 = 120 (m^*/m) \text{ A/cm}^2\text{-K}^2$ is Richardson's constant, Φ_B is the barrier height, and n is the ideality factor.

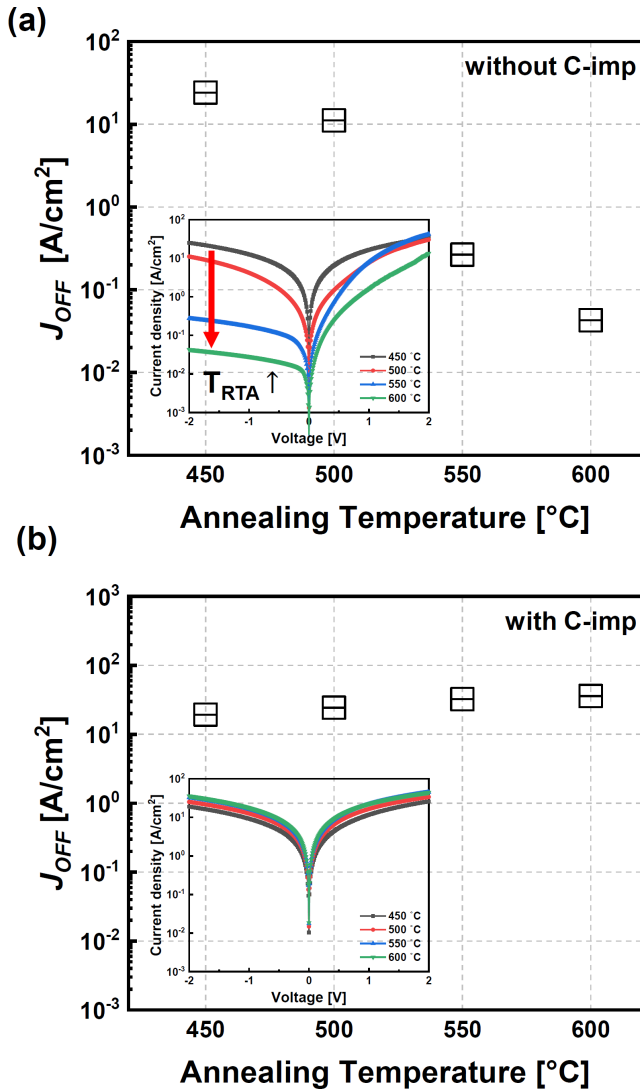


FIGURE 1. J_{OFF} of Ti/TiO₂/n-Ge contacts (a) without and (b) with C-imp after RTA at 450–600 °C for 60 s in N₂ ambient. Inset: corresponding $J-V$ curves at various RTA temperatures.

For $V \gg kT/q$, equation (1) can be written as follows:

$$\ln(I/T^2) = \ln(AA^*) - q(\phi_B - V/n)/kT \quad (2)$$

$$\begin{aligned} \phi_B &= \frac{V}{n} - \frac{k d [\ln(I/T^2)]}{q d(1/T)} \\ &= \frac{V}{n} - \frac{2.3 k d [\log(I/T^2)]}{q d(1/T)} \end{aligned} \quad (3)$$

The barrier height is calculated from the slope ($d[\ln(I/T^2)]/d(1/T)$) using bandgap energy (E_g) of 0.66 and an electron affinity (χ) of 4.0 eV for Ge at 300 K.

Fig. 2 shows the calculated SBH of Ti/TiO₂/n-Ge after RTA. Without C-imp, the SBH is constant at ~0.35 eV below 500 °C. Above 550 °C, the SBH increases and enters into the FLP regime. Such SBH degradation is attributed to the decomposition of the TiO₂ interlayer at the MS interfaces. With C-imp, the SBH is constant up to 600 °C. This suggests

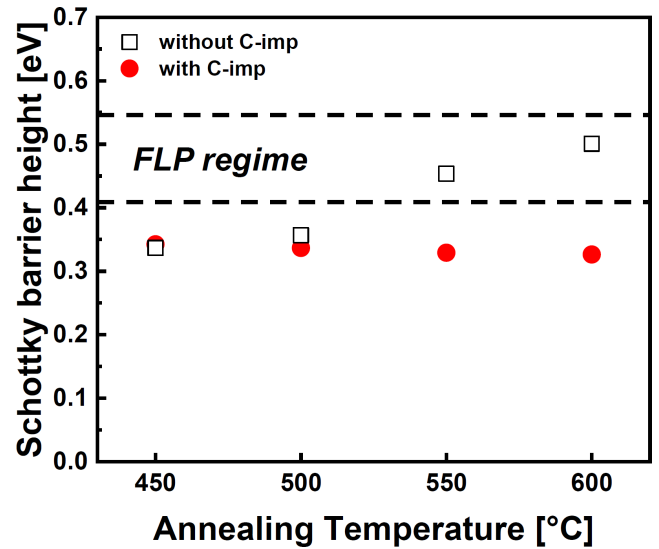


FIGURE 2. SBH of the Ti/TiO₂/n-Ge contacts without (black rectangle) and with (red circle) C-imp after RTA at 450–600 °C.

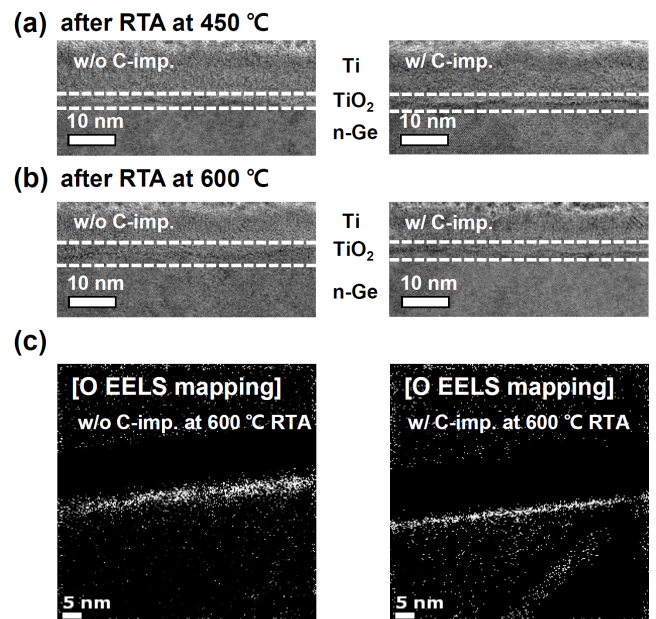


FIGURE 3. Cross-sectional TEM images of the Ti/TiO₂/n-Ge contacts without and with C-imp after RTA at (a) 450 and (b) 600 °C, and (c) the corresponding EELS maps for oxygen after RTA at 600 °C.

that FLP is suppressed in the MIS structure even after RTA temperatures above 550 °C.

Cross-sectional TEM images and EELS maps were used to understand the effect of the RTA temperature on the $J-V$ and SBH behaviors. After RTA at 450 °C, there is no deformation of TiO₂ layer irrespective of C-imp, as shown in Fig. 3(a). However, after RTA at 600 °C, the TiO₂ layer without C-imp becomes faint because of decomposition. This can be suppressed with C-imp, as shown in Fig. 3(b). Fig. 3(c) shows the EELS maps of oxygen for the Ti/TiO₂/n-Ge structures. The bright regions represent the areas with abundant oxygen.

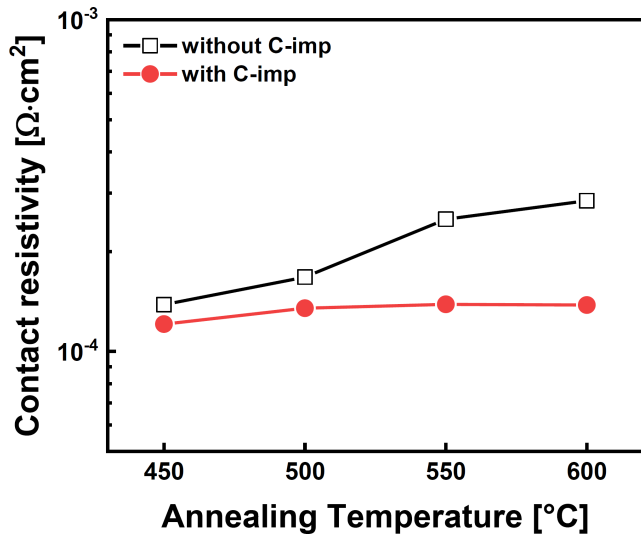


FIGURE 4. ρ_c of Ti/TiO₂/n-Ge contacts without (black curve) and with (red curve) C-imp as a function of RTA temperature.

The TiO₂ layer in Ti/TiO₂/n-Ge without C-imp is thicker than that in Ti/TiO₂/n-Ge with C-imp. This indicates that C-imp effectively reduces the out-diffusion of oxygen from the TiO₂ layer up to an RTA temperature of 600 °C.

Fig. 4 shows the ρ_c values obtained using the CTLM test structure versus the RTA temperature. At 600 °C, the ρ_c value of the sample without C-imp is similar to that of the Ti/n-Ge MS contact. This suggests that the TiO₂ layer collapses and the MIS structure changes to an MS-like structure. The ρ_c value of the Ti/TiO₂/n-Ge contact with C-imp is constant ($\sim 1.3 \times 10^{-4} \Omega \cdot \text{cm}^2$) up to 600 °C.

Thus, carbon incorporation effectively improves the thermal stability of the TiO₂ layer, thereby enhancing the electrical characteristics of the Ti/TiO₂/n-Ge contact.

IV. CONCLUSION

We experimentally demonstrated the effects of carbon incorporation on the electrical characteristics and thermal stability of the TiO₂ interfacial layer for Ti/TiO₂/n-Ge contacts. The MIS contact degraded at an RTA temperature above 550 °C. This degradation was caused by the deformation of TiO₂, which was confirmed through TEM images and EELS maps. Carbon incorporation effectively improved the thermal stability of TiO₂ with RTA. With C-imp, the SBH and ρ_c were relatively constant up to an RTA temperature of 600 °C. Thus, carbon incorporation effectively improves the thermal stability of MIS contacts, which can help develop high-performance Ge-based devices.

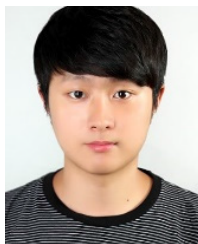
REFERENCES

- [1] D. P. Brunco et al., "Germanium MOSFET devices: Advances in materials understanding, process development, and electrical performance," *J. Electrochem. Soc.*, vol. 155, no. 7, pp. H552–H561, 2008, doi: 10.1149/1.2919115.
- [2] H. Kim, C. O. Chui, K. Saraswat, and P. C. McIntyre, "Local epitaxial growth of ZrO₂ on Ge (100) substrates by atomic layer epitaxy," *Appl. Phys. Lett.*, vol. 83, p. 2647, Sep. 2003, doi: 10.1063/1.1613031.

- [3] H. Shang, H. Okorn-Schmidt, J. Ott, P. Kozlowski, S. Steen, E. C. Jones, H.-S.-P. Wong, and W. Hanesch, "Electrical characterization of germanium p-channel MOSFETs," *IEEE Electron Device Lett.*, vol. 24, no. 4, pp. 242–244, Apr. 2003, doi: 10.1109/LED.2003.810879.
- [4] P. Tsouroutas, D. Tsoukalas, I. Zergioti, N. Cherkashin, and A. Claverie, "Modeling and experiments on diffusion and activation of phosphorus in germanium," *J. Appl. Phys.*, vol. 105, no. 9, May 2009, Art. no. 094910, doi: 10.1063/1.3117485.
- [5] F. A. Trumbore, "Solid solubilities of impurity elements in germanium and silicon," *Bell Syst. Tech. J.*, vol. 39, no. 1, pp. 205–233, Jan. 1960, doi: 10.1002/j.1538-7305.1960.tb03928.x.
- [6] E. Simoen and C. Claeys, *Germanium-Based Technologies*, 1st ed. Amsterdam, The Netherlands: Elsevier, 2007.
- [7] J. Robertson, Y. Guo, Z. Zhang, and H. Li, "Extending the metal-induced gap state model of Schottky barriers," *J. Vac. Sci. Technol. B, Microelectron.*, vol. 38, no. 4, Jul. 2020, Art. no. 042208, doi: 10.1116/6.0000164.
- [8] A. Dimoulas, P. Tsipas, A. Sotiropoulos, and E. K. Evangelou, "Fermi-level pinning and charge neutrality level in germanium," *Appl. Phys. Lett.*, vol. 89, Dec. 2006, Art. no. 252110, doi: 10.1063/1.2410241.
- [9] T. Nishimura, K. Kita, and A. Toriumi, "Evidence for strong Fermi-level pinning due to metal-induced gap states at metal/germanium interface," *Appl. Phys. Lett.*, vol. 91, no. 12, Sep. 2007, Art. no. 123123, doi: 10.1063/1.2789701.
- [10] G. Shine and K. C. Saraswat, "Analysis of atomistic dopant variation and Fermi level depinning in nanoscale contacts," *IEEE Trans. Electron Devices*, vol. 64, no. 9, pp. 3768–3774, Sep. 2017, doi: 10.1109/TED.2017.2720183.
- [11] G.-S. Kim, S.-H. Kim, T. Lee, B. Cho, C. Choi, C. Shin, J. Shim, J. Kim, and H. Y. Yu, "Fermi-level unpinning technique with excellent thermal stability for n-type germanium," *ACS Appl. Mater. Interfaces*, vol. 9, no. 41, pp. 35988–35997, Sep. 2017, doi: 10.1021/acsami.7b10346.
- [12] A. Agrawal, J. Lin, M. Barth, R. White, B. Zheng, S. Chopra, S. Gupta, K. Wang, J. Gelatos, S. E. Mohney, and S. Datta, "Fermi level depinning and contact resistivity reduction using a reduced titania interlayer in n-silicon metal-insulator-semiconductor ohmic contacts," *Appl. Phys. Lett.*, vol. 104, no. 11, Mar. 2014, Art. no. 112101, doi: 10.1063/1.4868302.
- [13] J.-Y. Lin, A. M. Roy, and K. C. Saraswat, "Reduction in specific contact resistivity to n⁺ Ge using TiO₂ interfacial layer," *IEEE Electron Device Lett.*, vol. 33, no. 11, pp. 1541–1543, Nov. 2012, doi: 10.1109/LED.2012.2214758.
- [14] N. Jain, Y. Zhu, D. Maurya, R. Varghese, S. Priya, and M. K. Hudait, "Interfacial band alignment and structural properties of nanoscale TiO₂ thin films for integration with epitaxial crystallographic oriented germanium," *J. Appl. Phys.*, vol. 115, no. 2, Jan. 2014, Art. no. 024303, doi: 10.1063/1.4861137.
- [15] J.-C. Yang, H.-F. Huang, J.-H. Li, Y.-J. Lee, and Y.-H. Wang, "Nitrogen plasma treatment of a TiO₂ layer for MIS ohmic contact on n-type Ge substrate," *Vacuum*, vol. 171, Jan. 2020, Art. no. 108996, doi: 10.1016/j.vacuum.2019.108996.
- [16] D. Biswas, J. Biswas, S. Ghosh, B. Wood, and S. Lodha, "Enhanced thermal stability of Ti/TiO₂/n-Ge contacts through plasma nitridation of TiO₂ interfacial layer," *Appl. Phys. Lett.*, vol. 110, no. 5, Jan. 2017, Art. no. 052104, doi: 10.1063/1.4974854.
- [17] G.-S. Kim, G. Yoo, Y. Seo, S.-H. Kim, K. Cho, B. J. Cho, C. Shin, J.-H. Park, and H.-Y. Yu, "Effect of hydrogen annealing on contact resistance reduction of metal–interlayer–n-germanium source/drain structure," *IEEE Electron Device Lett.*, vol. 37, no. 6, pp. 709–712, Jun. 2016, doi: 10.1109/LED.2016.2558582.
- [18] I. Park, D. Lee, B. Jin, J. Kim, and J.-S. Lee, "Improvement of Fermi-level pinning and contact resistivity in Ti/Ge contact using carbon implantation," *Micromachines*, vol. 13, no. 1, p. 108, Jan. 2022, doi: 10.3390/mi13010108.
- [19] H. Yu, M. Schaeckers, T. Schram, S. Demuyne, N. Horiguchi, K. Barla, N. Collaert, A. V.-Y. Thean, and K. De Meyer, "Thermal stability concern of metal-insulator-semiconductor contact: A case study of Ti/TiO₂/n-Si contact," *IEEE Trans. Electron Devices*, vol. 63, no. 7, pp. 2671–2676, Jul. 2016, doi: 10.1109/LED.2016.2565565.
- [20] D. David, G. Beranger, and E. A. Garcia, "A study of the diffusion of oxygen in α -titanium oxidized in the temperature range 460 °C–700 °C," *J. Electrochem. Soc.*, vol. 130, no. 6, pp. 1423–1426, Jun. 1983, doi: 10.1149/1.2119966.
- [21] M. Wittmer, J. Noser, and H. Melchior, "Oxidation kinetics of TiN thin films," *J. Appl. Phys.*, vol. 52, no. 11, p. 6659, 1981, doi: 10.1063/1.328659.
- [22] D. K. Schroder, *Semiconductor Material and Device Characterization*, 3rd ed. Hoboken, NJ, USA: Wiley, 2015.



IKSOO PARK (Student Member, IEEE) received the M.S. degree in electrical engineering (EE) from the Pohang University of Science and Technology (POSTECH), where he is currently pursuing the Ph.D. degree. He is focusing on advanced source and drain contact engineering for next-generation devices.



SEONGHWAN SHIN (Student Member, IEEE) received the M.S. degree in electrical engineering (EE) from the Pohang University of Science and Technology (POSTECH), where he is currently pursuing the Ph.D. degree. He is focusing on nano-scaled electronic devices and the bio sensor applications.



JUNGSIK KIM (Member, IEEE) received the Ph.D. degree in IT convergence engineering from the Pohang University of Science and Technology, Pohang, South Korea, in 2016.

He worked at SK-Hynix, from February 2016 to March 2018, for modeling of 96-stacks VNAND, and Samsung Electronics, from April 2019 to February 2020, for compact modeling of 1a-node DRAM. He was a Visiting Scholar with the NASA Ames Research Center, from April 2018 to March 2019, for reliability due to radiation effect in silicon devices. He is currently an Assistant Professor with the Department of Electrical Engineering, Gyeongsang National University, Jinju-si, South Korea. His research interests include the modeling and reliability of nano-scale devices based on technical computer-aided simulation and measurement.



BO JIN (Member, IEEE) received the B.S. degree in electrical communication engineering from the Yanbian University of Science and Technology (YUST), Yanji, China, in 2009, and the Ph.D. degree in IT convergence engineering from the Pohang University of Science and Technology (POSTECH), Pohang, Republic of Korea, in 2015. From 2015 to 2020, he worked as a Research Assistant Professor in electrical engineering at POSTECH. From 2020 to 2021, he joined the SJTU-Pinghu Institute of Intelligent Optoelectronics, China, and worked as a Visiting Experts and a Director Engineer. He has been working as a Senior Power Device Design Engineer at SPARC Company Ltd., China, since 2021. His current research interests include power device, nanoscale materials and devices, and biosensor and chemical sensor applications.



JEONG-SOO LEE (Senior Member, IEEE) received the B.S., M.S., and Ph.D. degrees in electrical engineering from the Pohang University of Science and Technology (POSTECH), South Korea, in 1991, 1993, and 1996, respectively. In 1996, he joined Samsung Electronics and worked as a Senior Engineer on the development of logic devices and nonvolatile memory devices. He was a Visiting Scholar at UC Berkeley, in 2001, where he developed Fin-FETs and ultra-thin-body (UTB) FETs. In 2005, he was a Founding Member of the National Center of Nanomaterials Technology (NCNT) established by the Ministry of Knowledge Economy, South Korea. Since 2008, he has been a Full Professor with the Department of Electrical Engineering, POSTECH; and also worked as the Vice-Director of NCNT. His research interests include Si-based nonplanar transistors, nanoscale devices, bottom-up nanowire transistors, and their biosensor applications.

...